



ChemComm

**Cobalt Amine Complexes and Ru265 Interact with the DIME  
Region of the Mitochondrial Calcium Uniporter**

Journal:	<i>ChemComm</i>
Manuscript ID	CC-COM-03-2021-001623.R1
Article Type:	Communication

SCHOLARONE™  
Manuscripts

## COMMUNICATION

## Cobalt Amine Complexes and Ru265 Interact with the DIME Region of the Mitochondrial Calcium Uniporter

Joshua J. Woods,<sup>a,b</sup> Madison X. Rodriguez,<sup>c</sup> Chen-Wei Tsai,<sup>c</sup> Ming-Feng Tsai<sup>c</sup> and Justin J. Wilson<sup>\*a</sup>Received 00th January 20xx,  
Accepted 00th January 20xx

DOI: 10.1039/x0xx00000x

**We report our investigation into the MCU-inhibitory activity of Co<sup>3+</sup> complexes in comparison to Ru265. These compounds reversibly inhibit the MCU with nanomolar potency. Mutagenesis studies and molecular docking simulations suggest that the complexes operate through interactions with the DIME motif of the MCU pore.**

Mitochondrial calcium (mt-Ca<sup>2+</sup>) ion uptake plays a critical role in a wide range of cellular signaling and bioenergetic processes.<sup>1–3</sup> These ions enter the mitochondria via the highly selective channel known as the mitochondrial calcium uniporter complex, which is composed of the pore-forming mitochondrial calcium uniporter subunit (MCU), and the regulatory EMRE, MICU1, and MICU2 subunits.<sup>4–7</sup> Dysregulation of Ca<sup>2+</sup> uptake through the MCU can have deleterious effects on cellular function and energy production.<sup>8–13</sup> As such, extensive efforts to develop new pharmacological strategies for modulating MCU activity have been undertaken with the purpose of identifying new tools and therapeutic agents for understanding and protecting against abnormal mt-Ca<sup>2+</sup> dynamics.<sup>10,14</sup> This work has led to the discovery of several organic<sup>15–20</sup> and inorganic<sup>21–25</sup> compounds that inhibit MCU-mediated mt-Ca<sup>2+</sup> uptake. In addition to these well-known inhibitors, several studies have shown that a series of simple Co<sup>3+</sup> ammine (NH<sub>3</sub>) and amine complexes (Chart 1) are also MCU inhibitors.<sup>22,26,27</sup> Although these compounds displayed promising MCU-inhibitory effects in isolated mitochondria, no further efforts have been made to understand their mechanisms of action or their ability to operate in intact cellular systems. In contrast to the majority of known MCU inhibitors, these simple Co<sup>3+</sup> complexes are easy to synthesize and purify, and do not appear to possess detrimental biological effects, such as cytotoxicity. These advantages make

these compounds appealing candidates as tools for studying mt-Ca<sup>2+</sup> dynamics. In this manuscript, we investigate this class of complexes as MCU inhibitors. Through this work, we have identified two complexes, [Co(en)<sub>3</sub>]<sup>3+</sup> (**3**, en = ethylenediamine) and [Co(sep)]<sup>3+</sup> (**6**, sep = 1,3,6,8,10,13,16,19-octaazabicyclo[6.6.6]eicosane) to be potent MCU inhibitors and have evaluated their biological activity in comparison to Ru265 (Chart 1).<sup>21,28</sup> These findings highlight the utility of simple Co<sup>3+</sup> complexes as readily accessible and affordable tools for studying mt-Ca<sup>2+</sup> dynamics in permeabilized cells and isolated mitochondria.

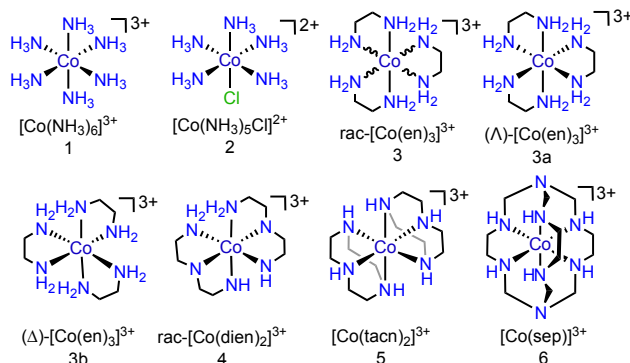


**Chart 1.** Chemical structures of Co<sup>3+</sup> complexes investigated in this study.

We initially screened the mt-Ca<sup>2+</sup> uptake-inhibitory properties of the Co<sup>3+</sup> complexes shown in Chart 1 in digitonin-permeabilized HeLa cells incubated with the Ca<sup>2+</sup>-responsive fluorescent indicator Calcium Green-5N at concentrations of 10 and 50 μM.<sup>25,28</sup> In the presence of 10 μM of either [Co(NH<sub>3</sub>)<sub>6</sub>]<sup>3+</sup> (**1**), *rac*-[Co(en)<sub>3</sub>]<sup>3+</sup> (**3**, *rac* = racemic), or [Co(sep)]<sup>3+</sup> (**6**), mt-Ca<sup>2+</sup> uptake is inhibited by ≥ 50% compared to untreated cells. The remaining complexes were found to be less active, showing negligible inhibitory action at 10 μM (Figures S1 – S2).

Having identified complexes **1**, **3**, and **6** to be effective inhibitors of mt-Ca<sup>2+</sup> uptake, we performed a dose-response study to determine their relative potencies in comparison to the known MCU inhibitor Ru265 in both permeabilized HeLa and

<sup>a</sup> Department of Chemistry and Chemical Biology, Cornell University, Ithaca, NY, USA

<sup>b</sup> Robert F. Smith School for Chemical and Biomolecular Engineering, Cornell University, Ithaca, NY, USA.

<sup>c</sup> Department of Physiology and Biophysics, University of Colorado Anschutz Medical Campus, Aurora, CO, USA.

\*corresponding author: jjw275@cornell.edu

Electronic Supplementary Information (ESI) available: See DOI: 10.1039/x0xx00000x

HEK293T cells (Table 1, Figures S3 – S8). We found complex **3** to be the most potent  $\text{Co}^{3+}$ -based MCU inhibitor with a 50% inhibitory concentration ( $\text{IC}_{50}$ ) of 115 nM in HeLa cells and 76 nM in HEK293T cells (Table 1, Figures S5 and S7). Importantly, free ethylenediamine does not appreciably inhibit mt- $\text{Ca}^{2+}$  uptake at concentrations lower than 500  $\mu\text{M}$ , suggesting that the intact  $\text{Co}^{3+}$  complex is required for MCU inhibition (Figure S9). Because **3** can exist as two different enantiomers, ( $\Lambda$ )- $[\text{Co}(\text{en})_3]^{3+}$  (**3a**) and ( $\Delta$ )- $[\text{Co}(\text{en})_3]^{3+}$  (**3b**), we also tested the ability of the optically pure isomers to inhibit the MCU and found both isomers to be comparably potent inhibitors of mt- $\text{Ca}^{2+}$  uptake (Table 1, Figure S8). Even though complexes **3** and **6** are less potent than the ruthenium-based MCU inhibitor Ru265 (Table 1),<sup>21,28,29</sup> their nM-inhibitory activity of mt- $\text{Ca}^{2+}$  uptake still renders them interesting candidates for this application. As such, we sought to further study their biological activity and explore how they inhibit the MCU.

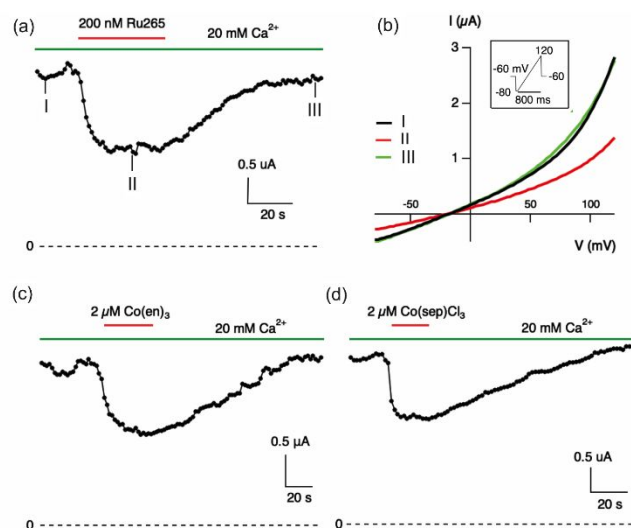
**Table 1.**  $\text{IC}_{50}$  values of Ru265 and  $\text{Co}^{3+}$  complexes for mitochondrial  $\text{Ca}^{2+}$  uptake inhibition in permeabilized HeLa ( $5 \times 10^6$  cells  $\text{mL}^{-1}$ ) and HEK293T ( $1 \times 10^7$  cells  $\text{mL}^{-1}$ ) cells.

Complex	$\text{IC}_{50}$ HeLa (nM)	$\text{IC}_{50}$ HEK293T (nM)
Ru265	$3.9 \pm 1$	$8.6 \pm 2.2$
$[\text{Co}(\text{NH}_3)_6]^{3+}$ ( <b>1</b> )	$20000 \pm 4000$	-
<i>rac</i> - $[\text{Co}(\text{en})_3]^{3+}$ ( <b>3</b> )	$115 \pm 13$	$76 \pm 10$
( $\Lambda$ )- $[\text{Co}(\text{en})_3]^{3+}$ ( <b>3a</b> )	$132 \pm 14$	-
( $\Delta$ )- $[\text{Co}(\text{en})_3]^{3+}$ ( <b>3b</b> )	$118 \pm 6$	-
$[\text{Co}(\text{sep})]^{3+}$ ( <b>6</b> )	$181 \pm 35$	$131 \pm 21$

Following our experiments with permeabilized cells, we next examined the cellular activity of **3** and **6** in an intact cell system. All of the complexes were found to be only moderately toxic below 500  $\mu\text{M}$  in HEK293T and HeLa cells, decreasing cell viability by approximately 50% at the highest concentration tested (Figure S10). Furthermore, these compounds do not negatively affect the mitochondrial membrane potential as measured by the JC-1 assay (Figures S11 – S13). The cellular uptake of the complexes, measured by graphite furnace atomic absorption spectroscopy, reveals that they are able to effectively cross the cell membrane (Figure S14). Encouraged by the cell-permeability and low toxicity of these compounds, we examined the ability of **3** and **6** to inhibit mt- $\text{Ca}^{2+}$  uptake in intact cells using the fluorescent  $\text{Ca}^{2+}$  indicator Rhod2AM.<sup>30</sup> Cells were treated with the metal complex (50  $\mu\text{M}$ ) for 1 h before being loaded with the dye. Mitochondrial calcium uptake was stimulated using histamine (100  $\mu\text{M}$ ), and the fluorescence response of the dye was taken as a direct readout of mt- $\text{Ca}^{2+}$  levels. Cells incubated with Ru265 show significantly reduced mt- $\text{Ca}^{2+}$  uptake compared to control cells, confirming previous reports that this complex inhibits the MCU in intact cell systems (Figure S15).<sup>21,29,31,32</sup> By contrast, cells treated with **3** and **6** do not show any reduction in mt- $\text{Ca}^{2+}$  accumulation, suggesting that these complexes are unable to inhibit the MCU in intact cells (Figure S15). The lack of inhibition by **3** and **6** in intact cells could be due to unfavourable intracellular localization that prevents them from reaching the MCU. To investigate this hypothesis, we treated cells with 50  $\mu\text{M}$  **3**, separated the mitochondrial and extramitochondrial

components, and measured the Co concentrations in each fraction by GFAAS. These results show that the mitochondria are not enriched in cobalt compared to the extramitochondrial fraction (Figure S16), suggesting that the intracellular distribution of these  $\text{Co}^{3+}$  compounds limits their MCU-binding in intact cells.

We next sought to explore the MCU-inhibitory mechanisms of Ru265, **3**, and **6**. We first tested the reversibility of MCU-inhibition by these compounds. To this end, a human MCU-EMRE fusion protein was expressed in *Xenopus* oocytes, and the outwardly-rectifying  $\text{Ca}^{2+}$ -activated  $\text{Cl}^-$  currents ( $I_{\text{CACC}}$ ) elicited by MCU-mediated inward  $\text{Ca}^{2+}$  currents were recorded via a two-electrode voltage clamp as established in our previous work.<sup>33</sup> The addition of Ru265 inhibits the MCU, as indicated by a reduction of  $I_{\text{CACC}}$  (Figure 1 a,b). Washing the oocytes with Ru265-free solutions induces a slow  $I_{\text{CACC}}$  current recovery to the original level with a time constant of  $\sim 20$  s, indicating that Ru265 inhibition of MCU is fully reversible (Figure 1 a,b). Similar observations were also made when the oocytes were treated with compounds **3** and **6** in an analogous procedure (Figure 1 c,d), demonstrating that the activities of these  $\text{Co}^{3+}$ -based

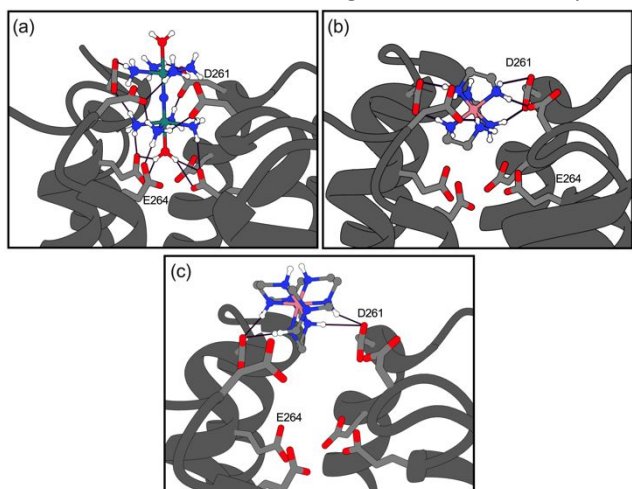


inhibitors are also reversible.

**Figure 1.** Electrical recordings of MCU activity. (a) Ru265 inhibition of MCU-induced  $I_{\text{CACC}}$  with currents at 120 mV plotted as a function of time. (b) The I-V relation of  $I_{\text{CACC}}$  in *Xenopus* oocytes treated with Ru265 at times indicated in panel a. (c,d) Inhibition of  $I_{\text{CACC}}$  by  $\text{Co}^{3+}$  complexes.

It has been established that the MCU pore, which possesses two transmembrane helices (TMH1 & TMH2), tetramerizes to form a  $\text{Ca}^{2+}$ -selective pore.<sup>34–37</sup> The TMH2 is the pore-lining helix containing a conserved DIME motif that forms the  $\text{Ca}^{2+}$  selectivity filter at the cytoplasmic entrance of the pore. The DIME-Asp, D261 in human MCU, is directly exposed to the intermembrane space, and has been identified as the binding site for the regulatory MICU1 subunit<sup>6,38,39</sup> and the MCU inhibitors Ru360 and mitoxantrone.<sup>16,34</sup> To predict the role of this residue on the inhibitory activities of Ru265, **3**, and **6**, we conducted docking studies using the DIME motif region as the search space. Because the chloride ligands of Ru265 are rapidly replaced by water in aqueous solution, we employed the aqua-capped analogue Ru265' instead.<sup>28</sup> The docking studies show

significant hydrogen-bonding interactions between Ru265' and both the DIME-Asp (D261) and -Glu (E264) of all four subunits of the MCU pore (Figures 2a and S16). In contrast to Ru265, our calculations predict that **3** and **6** only interact with the D261 of the MCU (Figures 2 b,c and S17). These results suggest that the enhanced potency of Ru265 compared to the mononuclear Co<sup>3+</sup> complexes, which is reflected by the higher docking score (Table S1), may be a consequence of its ability to participate in hydrogen-bonding interactions with both the aspartate and glutamate residues in all four subunits of the selectivity filter of the MCU. Notably, docking studies using the inactive compounds **1**, **2**, **4**, and **5** reveal the potential for similar types of interactions with the MCU as **3** and **6**. The lack of observed MCU-inhibitory activity of these compounds, therefore, may be a consequence of their poor selectivity for this channel, which prevents them from reaching it in sufficiently high



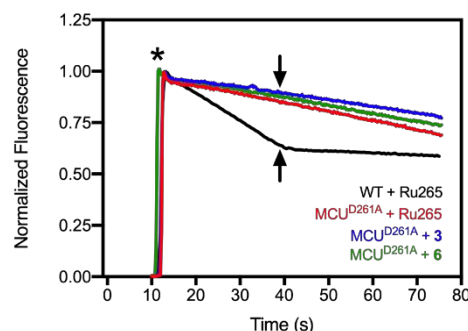
concentrations in the cellular milieu.

**Figure 2.** Molecular docking analysis of (a) Ru265', (b) **3**, and (c) **6** in the MCU (PDB 6O5B). Predicted hydrogen bonding interactions are shown as black lines. Atom colors: Green = Ru, Blue = N, Red = O, Pink = Co, White = H, Grey = C.

To validate the results of our docking studies, we studied the mt-Ca<sup>2+</sup> uptake in permeabilized, MCU-KO HEK293T cells transiently expressing wild-type (WT) or the MCU<sup>D261A</sup> mutant. As shown in Figure 3, the addition of 200 nM Ru265 to WT-MCU-expressing cells undergoing mt-Ca<sup>2+</sup> uptake leads to an immediate cessation of this process, confirming the rapid inhibitory effects of this compound. By contrast, when a 200 nM bolus of Ru265 is added to cells expressing the MCU<sup>D261A</sup> mutation, no change in the mt-Ca<sup>2+</sup> uptake transient is observed, indicating that the inhibitory activity of Ru265 is ablated by the D261A mutation. Similarly, the addition of **3** (2 μM) and **6** (2 μM) fails to elicit any changes of MCU<sup>D261A</sup>-mediated mt-Ca<sup>2+</sup> uptake, suggesting that D261 is also critically important for the inhibitory properties of these Co<sup>3+</sup> complexes. Thus, these results support the molecular docking studies implicating D261 as a site of interaction of these inhibitors. We previously found that single point mutation of a cysteine residue (C97) in the mitochondrial matrix-residing N-terminal domain of the MCU conferred resistance to inhibition by Ru265.<sup>21</sup> However, the interpretation of those previous experiments was complicated by the use of Ru265 at concentrations near the IC<sub>50</sub> for MCU inhibition and by the

expression of C97 mutants in HEK cells with native WT MCU. The current studies show that the D261 residue is critically important for the inhibitory activity of this compound, consistent with the findings that the structurally similar Ru360 inhibits MCU-mediated Ca<sup>2+</sup> uptake by binding to D261.<sup>34</sup> The docking studies (Figure 2), functional results (Figure 3), and the fact that D261 is exposed to the intermembrane space strongly argue that a direct interaction between Ru265 and D261 is significantly more likely than one between the matrix-exposed C97. These results provide compelling evidence that Ru265 and compounds **3** and **6** inhibit mt-Ca<sup>2+</sup> uptake through interactions with acidic amino acid residues located in the cytoplasmic entrance of the MCU pore.

The findings reported here establish [Co(en)<sub>3</sub>]<sup>3+</sup> (**3**) and [Co(sep)]<sup>3+</sup> (**6**) to be MCU inhibitors. Despite their high potency for MCU inhibition, these complexes lack the ability to inhibit mt-Ca<sup>2+</sup> uptake in intact cells, which may suggest low specificity of these compounds for the MCU or unfavourable intracellular speciation or localization. Electrical recording of MCU activity reveals that the inhibition of the MCU by these Co<sup>3+</sup> complexes and Ru265 is completely reversible, and site-directed mutagenesis studies highlight the role of the aspartate residue D261 as one of the potential active sites for inhibition of mt-Ca<sup>2+</sup> uptake. These results complement previous studies that reported the known MCU inhibitors Ru360 and mitoxantrone similarly inhibit mt-Ca<sup>2+</sup> uptake through interactions with D261,<sup>16,38</sup> and may suggest a common mechanism of action for inhibition of the MCU by these compounds. Knowledge of how these compounds inhibit mt-Ca<sup>2+</sup> uptake can potentially be



leveraged to the design of new MCU inhibitors.

**Figure 3.** Representative traces of extramitochondrial Ca<sup>2+</sup> clearance in HEK293T cells expressing either MCU<sup>WT</sup> or MCU<sup>D261A</sup> with addition of either 200 nM Ru265, 2 μM **3**, or 2 μM **6**. Addition of 15 μM Ca<sup>2+</sup> is indicated by \* and the arrow indicates addition of metal complex.

## Acknowledgements

This work was supported by the National Science Foundation (CHE-1750295) and a predoctoral fellowship to J.J. Woods from the American Heart Association (20PRE35120390). This study made use of the Cornell NMR facility, which is supported in part by the NSF (CHE-1531632), and the Cornell Institute of Biotechnology Imaging Facility, which is supported in part by the NIH (S10RR025502). Research in the lab of M. F. Tsai is supported by the NIH (R01-GM129345).

## Notes and references

- 1 D. E. Clapham, *Cell*, 2007, **131**, 1047–1058.
- 2 L. Contreras, I. Drago, E. Zampese and T. Pozzan, *Biochim. Biophys. Acta - Bioenerg.*, 2010, **1797**, 607–618.
- 3 J. R. Mickelson, *Meat Sci.*, 1983, **9**, 205–229.
- 4 S. Marchi and P. Pinton, *J. Physiol.*, 2014, **592**, 829–839.
- 5 M. Patron, V. Checchetto, A. Raffaello, E. Teardo, D. VecellioReane, M. Mantoan, V. Granatiero, I. Szabò, D. DeStefani and R. Rizzuto, *Mol. Cell*, 2014, **53**, 726–737.
- 6 M. Fan, J. Zhang, C.-W. Tsai, B. J. Orlando, M. Rodriguez, Y. Xu, M. Liao, M.-F. Tsai and L. Feng, *Nature*, 2020, **582**, 129–133.
- 7 K. J. Kamer and V. K. Mootha, *Nat. Rev. Mol. Cell Biol.*, 2015, **16**, 545–553.
- 8 A. Vultur, C. S. GIBHARDT, H. Stanisiz and I. Bogeski, *Pflügers Arch. J. Physiol.*, 2018, **470**, 1149–1163.
- 9 N. Nemani, S. Shanmughapriya and M. Madesh, *Cell Calcium*, 2018, **74**, 86–93.
- 10 D. M. Arduino and F. Perocchi, *J. Physiol.*, 2018, **596**, 2717–2733.
- 11 C. Mammucari, G. Gherardi and R. Rizzuto, *Front. Oncol.*, 2017, **7**, 139.
- 12 M. I. Faizan and T. Ahmad, *Mitochondrion*, 2021, **57**, 47–62.
- 13 C. V. Logan, G. Szabadkai, J. A. Sharpe, D. A. Parry, S. Torelli, A.-M. M. Childs, M. Kriek, R. Phadke, C. A. Johnson, N. Y. Roberts, D. T. Bonthron, K. A. Pysden, T. Whyte, I. Munteanu, A. R. Foley, G. Wheway, K. Szymanska, S. Natarajan, Z. A. Abdelhamed, J. E. Morgan, H. Roper, G. W. E. E. Santen, E. H. Niks, W. L. Van Der Pol, D. Lindhout, A. Raffaello, D. De Stefani, J. T. Den Dunnen, Y. Sun, I. Ginjaar, C. A. Sewry, M. Hurles, R. Rizzuto, M. R. Duchon, F. Muntoni and E. Sheridan, *Nat. Genet.*, 2014, **46**, 188–193.
- 14 J. J. Woods and J. J. Wilson, *Curr. Opin. Chem. Biol.*, 2020, **55**, 9–18.
- 15 N. Kon, M. Murakoshi, A. Isobe, K. Kagechika, N. Miyoshi and T. Nagayama, *Cell Death Discov.*, 2017, **3**, 17045.
- 16 D. M. Arduino, J. Wettmarshausen, H. Vais, P. Navas-Navarro, Y. Cheng, A. Leimpek, Z. Ma, A. Delrio-Lorenzo, A. Giordano, C. Garcia-Perez, G. Médard, B. Kuster, J. García-Sancho, D. Mokranjac, J. K. Foskett, M. T. Alonso and F. Perocchi, *Mol. Cell*, 2017, **67**, 711–723.
- 17 J. Schwartz, E. Holmuhamedov, X. Zhang, G. L. Lovelace, C. D. Smith and J. J. Lemasters, *Toxicol. Appl. Pharmacol.*, 2013, **273**, 172–179.
- 18 G. Di Marco, F. Vallese, B. Jourde, C. Bergsdorf, M. Sturlese, A. De Mario, V. Techer-Etienne, D. Haasen, B. Oberhauser, S. Schleegeer, G. Minetti, S. Moro, R. Rizzuto, D. De Stefani, M. Fornaro and C. Mammucari, *Cell Rep.*, 2020, **30**, 2321–2331.
- 19 V. T. Thu, H. K. Kim, L. T. Long, S. R. Lee, T. M. Hanh, T. H. Ko, H. J. Heo, N. Kim, S. H. Kim, K. S. Ko, B. D. Rhee and J. Han, *Cardiovasc. Res.*, 2012, **94**, 342–350.
- 20 J. Santo-Domingo, L. Vay, E. Hernández-Sanmiguel, C. D. Lobatón, A. Moreno, M. Montero and J. Alvarez, *Br. J. Pharmacol.*, 2007, **151**, 647–654.
- 21 J. J. Woods, N. Nemani, S. Shanmughapriya, A. Kumar, M. Zhang, S. R. Nathan, M. Thomas, E. Carvalho, K. Ramachandran, S. Srikantan, P. B. Stathopoulos, J. J. Wilson and M. Madesh, *ACS Cent. Sci.*, 2019, **5**, 153–166.
- 22 J. F. Unitt, K. L. Boden, A. V Wallace, A. H. Ingall, M. E. Coombs and F. Ince, *Bioorg. Med. Chem.*, 1999, **7**, 1891–1896.
- 23 M. A. Matlib, Z. Zhou, S. Knight, S. Ahmed, K. M. Choi, J. Krause-Bauer, R. Phillips, R. Altschuld, Y. Katsube, N. Sperelakis and D. M. Bers, *J. Biol. Chem.*, 1998, **273**, 10223–10231.
- 24 J. Emerson, M. J. Clarke, W. L. Ying and D. R. Sanadi, *J. Am. Chem. Soc.*, 1993, **115**, 11799–11805.
- 25 S. R. Nathan, N. W. Pino, D. M. Arduino, F. Perocchi, S. N. MacMillan and J. J. Wilson, *Inorg. Chem.*, 2017, **56**, 3123–3126.
- 26 B. A. Tashmukhamedov, A. I. Gagelgans, K. Mamatkulov and E. M. Makhmudova, *FEBS Lett.*, 1972, **28**, 239–242.
- 27 M. Crompton and L. Andreeva, *Biochem. J.*, 1994, **302**, 181–185.
- 28 J. J. Woods, J. Lovett, B. Lai, H. H. Harris and J. J. Wilson, *Angew. Chem. Int. Ed.*, 2020, **59**, 6482–6491.
- 29 R. J. Novorolsky, M. Nichols, J. S. Kim, E. V. Pavlov, J. J. Woods, J. J. Wilson and G. S. Robertson, *J. Cereb. Blood Flow Metab.*, 2020, **40**, 1172–1181.
- 30 A. Minta, J. P. Y. Kao and R. Y. Tsien, *J. Biol. Chem.*, 1989, **264**, 8171–8178.
- 31 M. Kerkhofs, R. La Rovere, K. Welkenhuysen, A. Janssens, P. Vandenberghe, M. Madesh, J. B. Parys and G. Bultynck, *Cell Calcium*, 2021, **94**, 102333.
- 32 T. E. Huntington and R. Srinivasan, *Cell Calcium*, 2021, **96**, 102383.
- 33 C. W. Tsai and M. F. Tsai, *J. Gen. Physiol.*, 2018, **150**, 1035–1043.
- 34 C. Fan, M. Fan, B. J. Orlando, N. M. Fastman, J. Zhang, Y. Xu, M. G. Chambers, X. Xu, K. Perry, M. Liao and L. Feng, *Nature*, 2018, **559**, 575–579.
- 35 N. X. Nguyen, J. P. Armache, C. Lee, Y. Yang, W. Zeng, V. K. Mootha, Y. Cheng, X. Bai and Y. Jiang, *Nature*, 2018, **559**, 570–574.
- 36 R. Baradaran, C. Wang, A. F. Siliciano and S. B. Long, *Nature*, 2018, **559**, 580–584.
- 37 J. Yoo, M. Wu, Y. Yin, M. A. Herzik, G. C. Lander and S.-Y. Lee, *Science*, 2018, **361**, 506–511.
- 38 M. Paillard, G. Csordás, K.-T. Huang, P. Várnai, S. K. Joseph and G. Hajnóczky, *Mol. Cell*, 2018, **72**, 778–785.
- 39 C. B. Phillips, C.-W. Tsai and M.-F. Tsai, *Elife*, 2019, **8**, e41112.